

REVERSE ENGINEERING OF PARTS WITH ASYMMETRICAL PROPERTIES USING REPLACEMENT MATERIALS

Mehmet ALADAG^{***}, Monika BERNACKA^{****}, Magdalena JOKA-YILDIZ^{****},
 Wojciech GRODZKI^{*}, Przemysław ZAMOJSKI^{*}, Izabela ZGŁOBICKA^{*}

^{*}Faculty of Mechanical Engineering, Białystok University of Technology, ul. Wiejska 45C, 15-351 Białystok, Poland

^{**}Faculty of Mechanical Engineering, Gaziantep University, Osmangazi, Üniversite Blv., 27410 Sehitkamil/Gaziantep, Turkiye

^{***}Technology Applied Sp. z o.o., ul. Wiejska 42/3, 15-509 Sobolewo, Poland

^{****}Faculty of Civil Engineering and Environmental Sciences, Białystok University of Technology, ul. Wiejska 45E, 15-351 Białystok, Poland

mmehmetaladag@gmail.com, monika6@wp.pl, m.joka@pb.edu.pl,
w.grodzki@pb.edu.pl, p.zamojski@doktoranci.pb.edu.pl, i.zglobicka@pb.edu.pl

received 17 March 2022, revised 31 May 2022, accepted 13 June 2022

Abstract: Reverse engineering (RE) aims at the reproduction of products following a detailed examination of their construction or composition. Nowadays, industrial applications of RE were boosted by combining it with additive manufacturing. Printing of reverse-engineered elements has become an option particularly when spare parts are needed. In this paper, a case study was presented that explains how such an approach can be implemented in the case of products with asymmetric mechanical properties and using replacement materials. In this case study, a reverse engineering application was conducted on a textile machine spare part. To this end, the nearest material was selected to the actual material selection and some mechanical tests were made to validate it. Next, a replacement part was designed by following the asymmetric push-in pull-out characteristic. Finally, the finite element analysis with Additive Manufacturing was combined and validated experimentally.

Keywords: material characterisation, reverse engineering, additive manufacturing, finite element analysis, rapid prototyping

1. INTRODUCTION

Reverse engineering (RE) is nowadays widely used for solving problems related to the fabrication of spare parts for devices already in use for which full technical documentation is no longer available and/or spare parts can hardly be found. The frequency of such situations is expected to be increasing in the coming years because of current trends for extending the service time of devices stimulated by environmental concerns (R3 principle: reduce, re-use, re-cycle) [1]. Moreover, the parts that are remanufactured with high-added value by various manufacturing methodologies have claimed to gain environmental benefits. Accordingly, comparing the life cycle assessment with the parts which are manufactured, remanufactured parts have the advantage regarding environmental attractiveness [2].

The popularity of RE has also increased with easier access to 3D printers, particularly using polymeric materials. However, standard printers are utilising a relatively low number of substrates, far lower than the number of construction and functional engineering materials. Thus, an efficient approach to RE and fabrication of replacement parts might require, in some cases, the use of replacement materials with properties differing from the ones used by a manufacturer of the original element [3].

In this case study of industrial importance, the selected replacement part is made from a rubber material since rubber as such is not as of yet a printing material [4–8]. Thermoplastic polyurethane (TPU) was selected as a replacement [9, 10], which

is an additively manufacturable material and has good material properties in terms of ductility, shock absorption resistance and excellent biomedical application compatibility [11–16]. There are several studies reported in the literature on the mechanical properties of elements made of TPU by additive manufacturing [17–19]. In addition, TPU allows for printing high-porous, low-density structures. Thus, functionally graded parts can be printed and by printing lattice type structures, elements of pre-defined stiffness can be produced [20–24].

The similar studies have been made by the researchers. Ponticelli et al. [25] studied the RE of an Impeller for submersible electric pump. In their study, an impeller was engineered by using RE techniques and fabricated by selective laser melting (SLM) method. In addition, Hernández and Fragoso [26] studied manufacture of a pump impeller by integration of 3D sand printing and casting. An impeller was scanned by 3D scanner. After that, the cavity geometry was manufactured by 3D sand printer by using binder jet printing method to make a casting operation. By following the casting steps, the part cast with a AISI 316 cast stainless steel. To obtain thin final geometry, a post-processing operation was made on the cast part and, thus, the final geometry was obtained.

In this paper, an approach was demonstrated that can be used to RE geometry (reproduction of size and shape) and material properties (reproduction properties using replacement materials) at the same time. The advantages of the approach proposed, which is based on Finite Element Modelling, are

demonstrated using a case study of industrial relevance. The current paper can also be viewed as presenting advantages of additive manufacturing (AM), in the fabrication of replacement parts, RP, in a wide range of industries [27–29].

2. PROBLEM DEFINITION

The proposed approach to RE allowed the use of replacement materials demonstrated for a rubber machine part as shown in Fig. 1. This is a textile machine yarn pass that has been damaged in extended in-service conditions.



Fig. 1. Damaged textile machine yarns pass analyzed

The original yarn pass was made of rubber, for which as of yet no 3D printing technology exists. In this situation, a decision was made to print the part in question using thermoplastic polyurethane, TPU. This is a block copolymer consisting of alternating sequences of hard segments (isocyanates) and soft segments (reacting polyol). Because of those properties, TPU can be shaped by adjusting the number of hard segments. Its hardness may range from 60A (similar to soft silicones) to 80D (equivalent to nylons or rigid PVC) [10]. In addition, it has good thermal stability and is quite easy to print using fused deposition modelling (FDM) or selective laser sintering (SLS) 3D printers. The SLS process has been chosen in the current case, which is considered a friendly manufacturing technique for plastic parts [30]. In addition, in the SLS method, complex parts can be fabricated without building support, printing time and cost. Also, the surface quality of the part manufactured by the SLS method is higher than the other 3D printing methods and does not require additional post-processing operation [31–33].

3. MATERIALS AND METHODS

3.1. Textile Machine Yarn Part Pass Geometry Engineering

The part was initially digitalized by a 3D scanner and, the dot clouds were generated. After that, it was converted to polygon and, exported polygon geometry as STL file format. Using NX 12 the part was re-designed with the tolerances ± 0.1 mm and, obtained a fully parametric solid model. The polygon model and solid model were given in Fig 2.

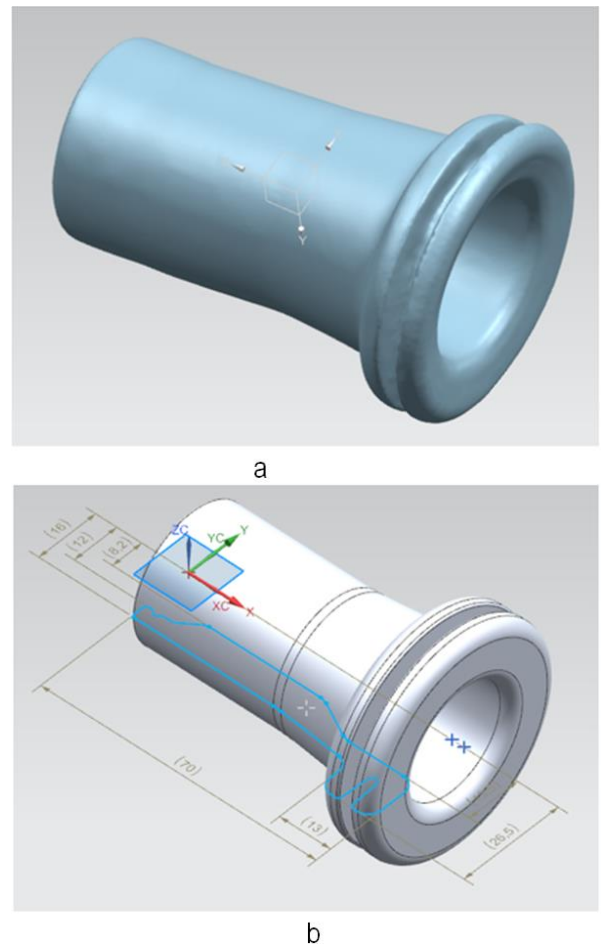


Fig 2. Textile machine yarn pass part; a) 3D scanned file polygon model, b) engineered solid model

3.2. Powder Characterisation

In this study, the TPU powder size distribution is a parameter in the context of selecting printing parameters. Accordingly, the size distribution of the powder was obtained with Analysette 22 MicroTec (Fritsch, Germany). For the same reasons, thermal properties of TPU used were investigated by a differential scanning calorimetry (DSC) and, thermogravimetric analysis (TGA). The thermal analyses were carried out using the TG 209 F1 Libra (Netsch, Germany) devices. Consequently, the powder shape is the last parameter that has significance in terms of the distribution quality on the bed. Thus, the powders were imaged under the Scios2 (ThermoFisher, USA) scanning electron microscopy (SEM). Results of the respective investigations are presented and results are discussed..

3.3. Part Characterisation

Replacement of original with some alternatives obviously requires thorough characteristics of materials considered. Usually, the needed characteristics were made available by materials suppliers. However, in the case of fabrication by 3D printing we should consider that the properties of printed material depend on the printing parameters. Thus, in order to replace the rubber part with TPU printed one, the mechanical properties of printed samples were measured in tensile and compression tests.

3.4. Tensile Test Specimen

Tensile tests specimens were prepared according to ISO 527-2 polymer tensile test standard [34] in the size and shape as given

in Fig. 3. The tensile tests samples were printed in two direction layouts; three of them are in the x-direction and, the others were in the y-directions as explained in Fig. 4.

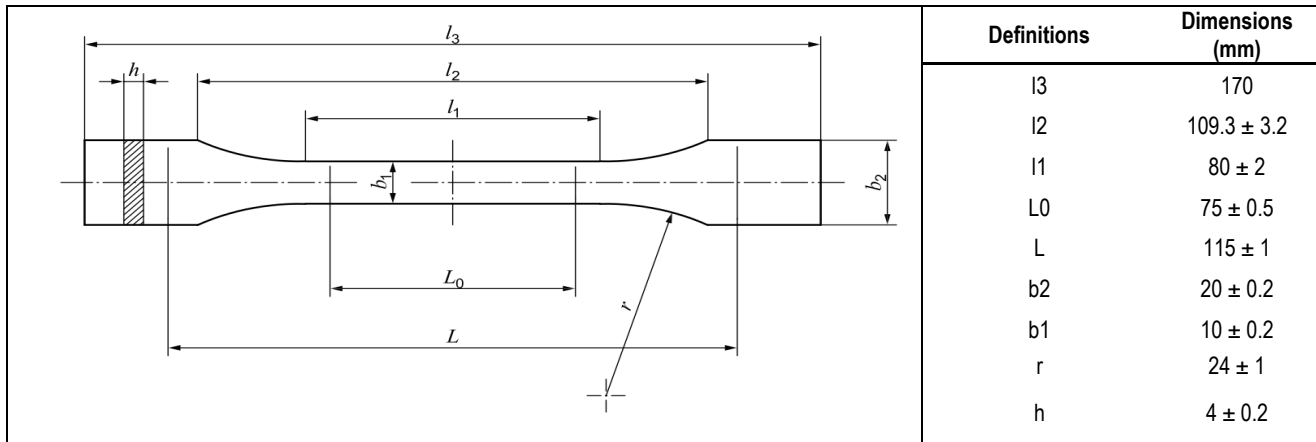


Fig. 3. Tensile test sample drawing and its dimensions

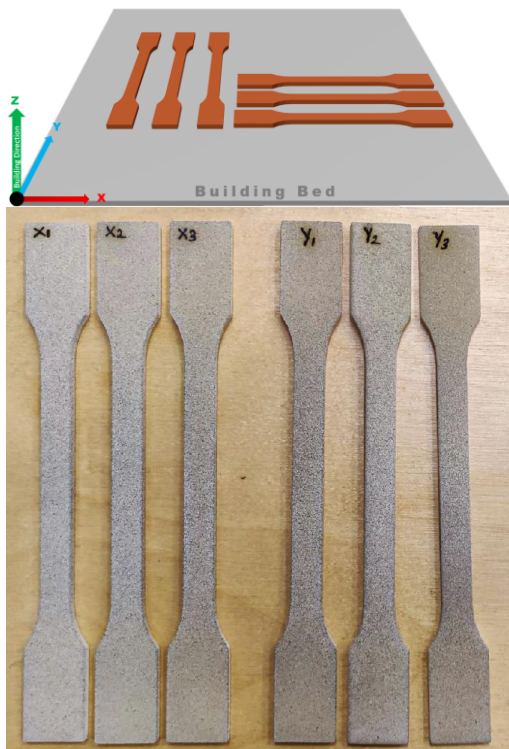


Fig. 4. Layout view on building table and specimens

3.5. Compression Test Specimen

In this study, two compression tests were conducted; one is full dense printed specimen and, the second one is lattice-type high porous specimen. The full dense printed specimen compression tests were conducted according to the ISO 7743 standard [35] using the specimens of width, height and depth of 10 ± 0.05 mm, shown in Fig. 5.

In addition to fully dense specimens, mechanical properties of lattice-type highly porous elements are also measured as shown in Fig. 6. The motivation for testing properties of such

structures was the recognition that TPU is significantly stiffer than the rubber used in the original part. Therefore, the replacement of rubber with TPU required a significant reduction in the stiffness which could be achieved by increasing its porosity [36]. To some degree, two specimens that have porous structures tested in this study can be viewed as a meta-material analogue of the rubber used in the original part.



Fig. 5. Compression test specimens

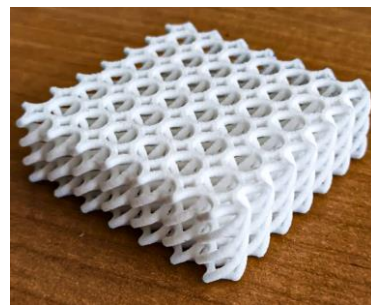


Fig. 6. An example of a highly porous element tested in compression tests

3.6. 3D Printing of the Samples

The specimens for testing mechanical properties were produced by SLS method. A 3D printer EOS P 396 was used, operated by Technology Applied Ltd. [37, 38]. The TPU powder

brand was TPU EOS 1301 white. In addition, the printing parameters were defined in accordance with the powder manufacturer catalogue. The catalogue information about SLS printer settings and TPU powder were given in Tab. 1 and 2.

Tab. 1. Printing parameters

Parameter	Unit	Value
Powder bed temperature	°C	108
Wavelength	µm	10.20–10.80
Process chamber	°C	108
Removal chamber	°C	60
Laser power	Watt	30
Laser scan speed	m/sec	5
Layer thickness	mm	0,1

Tab. 2. TPU Powder properties [39]

Parameter	Unit	Value
Melting temperature	°C	138
Bulk density	g/cm3	0.49
Flowability	s	17
Particle size d10	µm	22
Particle size d50	µm	72
Particle size d90	µm	138

3.7. FEM-Based Design Replacement Part

The model printed is engineered within the tolerances ± 0.1 mm by using NX 12. The engineered shape of the yarn pass is shown in Fig. 7. In the analytical part of designing, the inner and outer dimensions were kept fixed, and studied the performance of the spare part to-be-printed in the assembly process as well as its in-service stability.

The original part made of rubber was characterized by asymmetrical mechanical properties manifested by the difference encountered in push-in and pull-out actions. It is easy to insert and difficult to remove, assuring that it remains in a fixed position after installing. In the approach reported here, it is assumed that the required properties of the replacement part made of TPU can be obtained by printing an analogue that will contain specifically

located regions of high porosity. Also, the fish-bone concept is proposed to design the architecture of the porous regions. The fish-bone concept schematically was shown in Fig. 8.

An example of a design carried out in the study is shown in Fig. 9. It can be noted that the porous regions are placed in the external flange and that the cell-type architecture of these regions is highly anisotropic.



Fig. 7. The engineered views of textile yarn pass



Fig. 8. Fishbone geometry imparting asymmetric reaction of push-in and pull-out

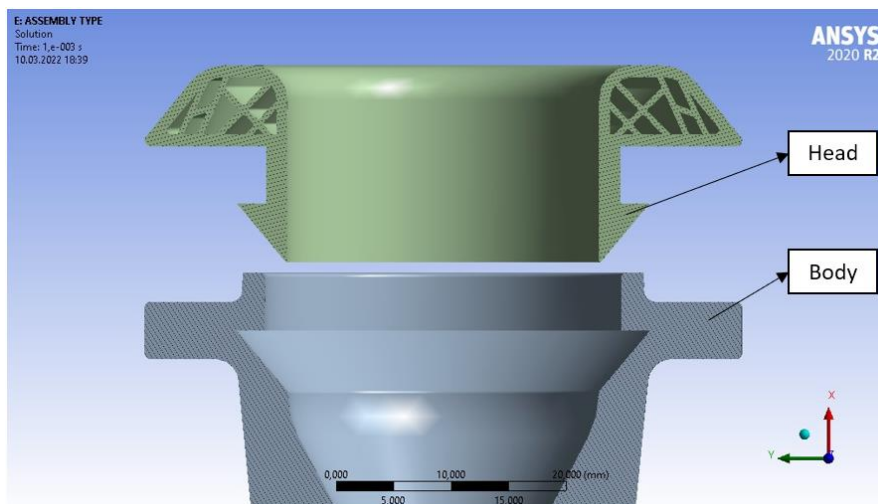


Fig. 9. An example of the design considered in the present study

4. RESULTS AND DISCUSSION

4.1. Characterisation of TPU powder

The TPU powder size distribution and representative SEM images were shown, respectively, in Fig. 10 and 11. It can be noted that the average size is exceeding 0.15 mm and the powder particles are irregular in shape. These two factors contribute to relatively rough surfaces of the prints obtained with this powder. However, high surface roughness in this case has no negative effect on the performance of the spare parts to be printed. Melting and glass transition temperatures estimated by DSC analysis, are 134 and 110°C, respectively (see Fig. 12). These two temperatures define ‘temperature window’ to be exploited in selecting the printing conditions.

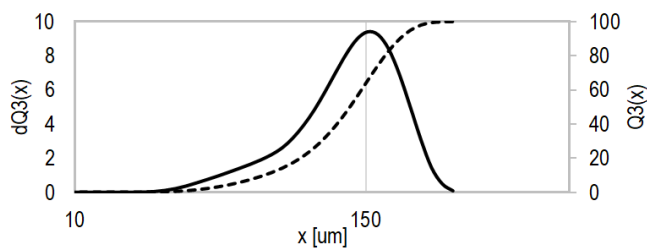


Fig. 10. Particle size distribution of TPU powder

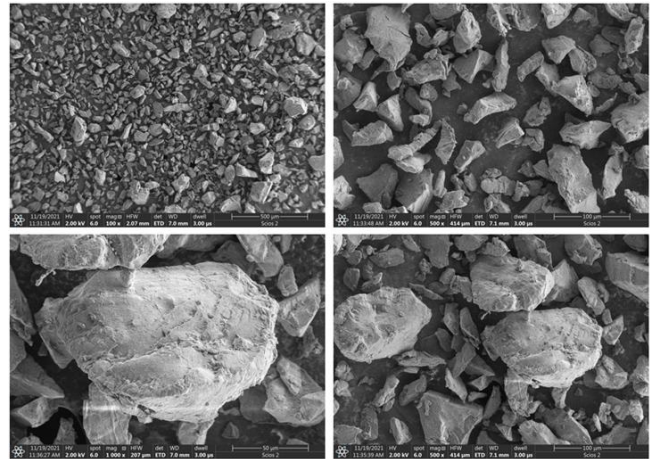


Fig. 11. SEM images of TPU powder shape

4.2. Full Dense Material Tension Test Results

Compression/tensile tests were conducted using the MTS Bionics machine and a video extensometer. The results of the tensile test of fully dense samples are shown in Fig. 13. The maximum stress value is approximately 6 MPa. The tensile modulus was calculated as 69.5 MPa. The manufacturer’s test values were maximum stress 7 MPa in X and Y-directions and, the tensile modulus was 70 MPa [39]. In addition, the Poisson’s ratio is calculated for each tensile specimen. The Fig. 14 shows that the average value of Poisson’s ratio is 0.48. It is seen that the Poisson’s ratio is also proper for general rubber material class.

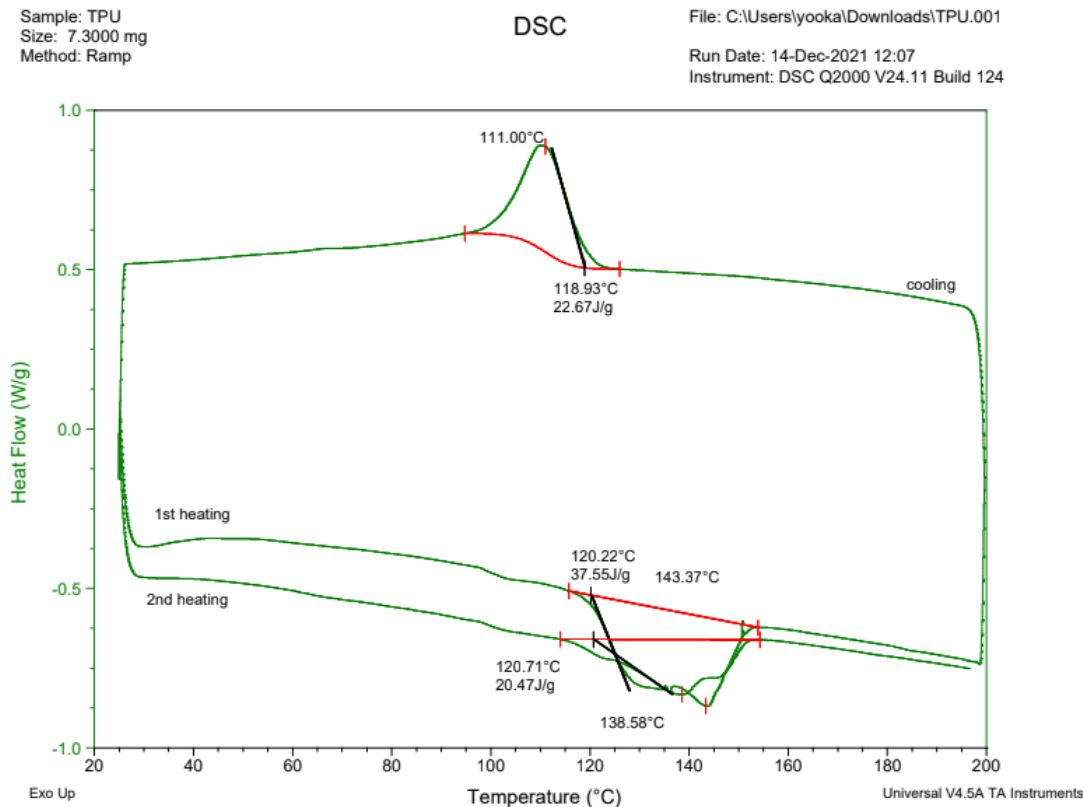


Fig. 12. DSC Scan of TPU powder

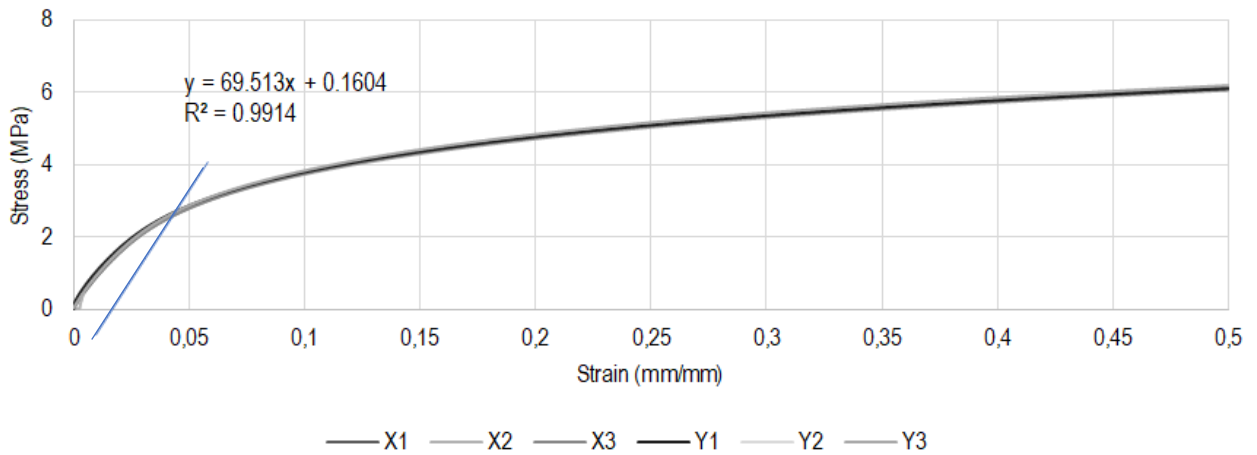


Fig. 13. Strain stress curves for fully dense printed samples of TPU

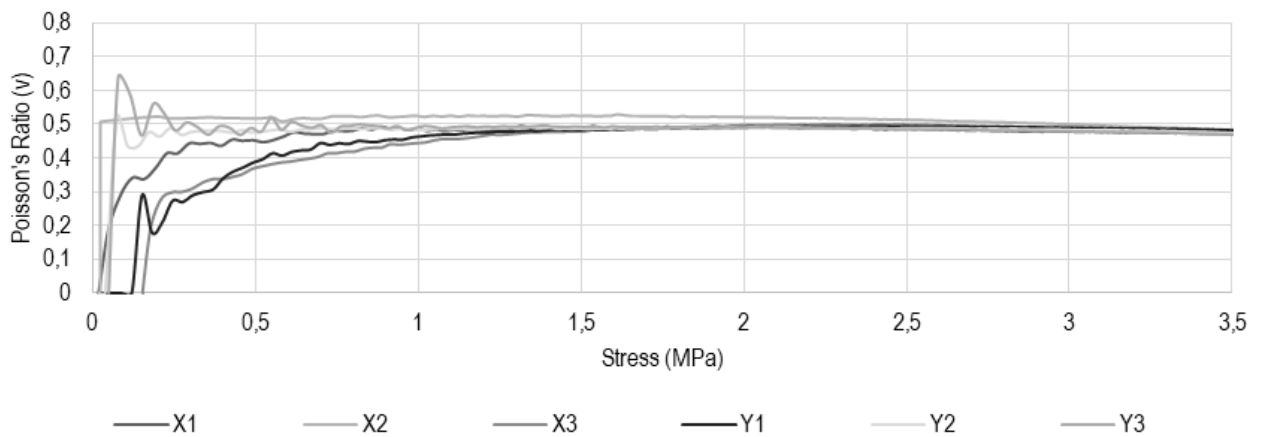


Fig. 14. The Poisson's curves for the specimens tested

4.3. Compression Test Results

The full dense printed sample compression tests were conducted in the MTS Bionics Tensile test machine on six same samples. The plotted stress-strain curves are in a great deal with all the compression test specimen. The load-displacement curve was given in Fig 15. The encountered stress is approximately 28 MPa. The values show that the specimens are stiffer under compressive load comparing to the tensile load. Further, the compressive stress value is approximately 4–5 times larger than the tensile strength.

Compression curves for highly porous structures are shown in

Fig. 16. The stress and strain have been calculated assuming the external dimensions of the specimens. The calculated stress value in the porous specimen is 0.058 MPa. It can be noted that the apparent stress is much lower than the full dense compression specimen.

Experimental Poisson number curves are plotted in Fig. 17. The curves have revealed some differences, which are expected for highly porous lattice-type prints. Nevertheless, one can assume that Poisson ratio of 0.07 can be used as an approximation for the samples obtained in the current study. Note that the latticed structure decreases the stiffness and the Poisson ratio significantly.

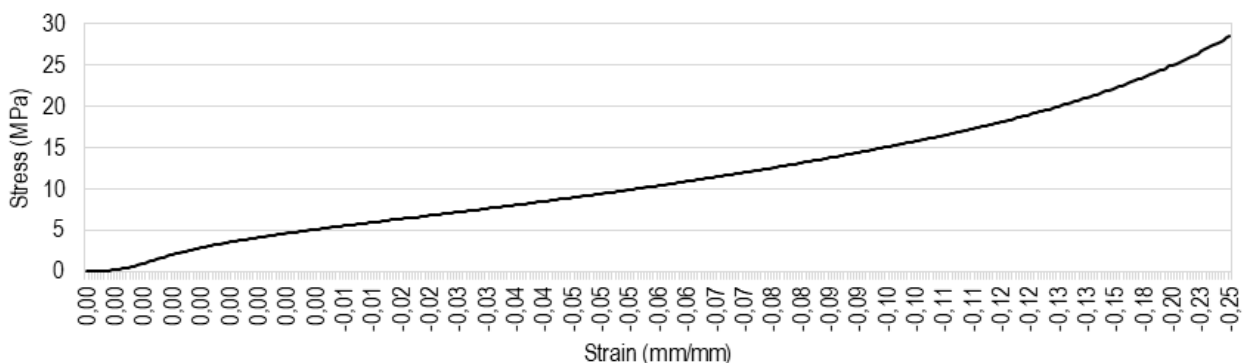


Fig 15. Stress-Strain curve of full dense printed material

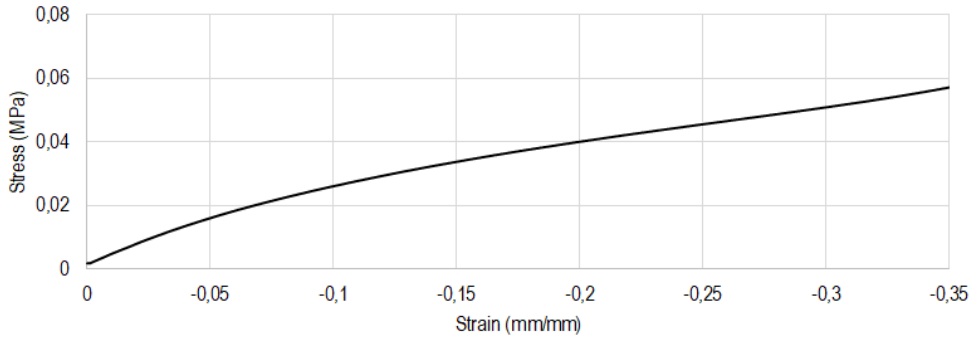


Fig. 16. Stress-strain curves for highly porous structure

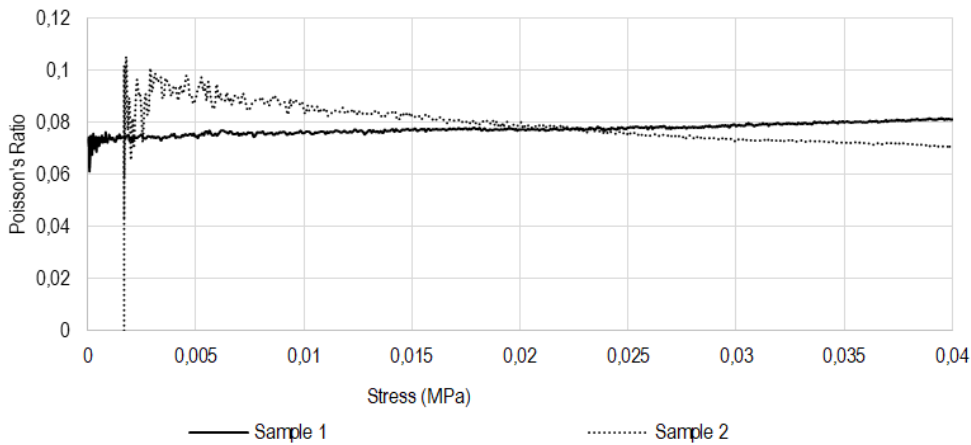


Fig. 17. The Poisson number curves for highly porous structure

4.4. FEA For Designed Replacement Part

The proposed replacement part has been analysed by finite element analysis (FEA) and the results obtained are given in Fig. 18. The equivalent maximum stress is seen not to exceed 5 MPa with the yield strength of the used TPU at 6 MPa. Hence, the maximum elastic strain is approximately 0.058 mm/mm. The value of average contact pressure is approximately 2 MPa. This also will

provide satisfying holding force after assembly. The old replacement part is made as a single part., which makes assembling difficult; it requires more force, and therefore, the part is deformed severely. Thus, the part has a high potential to deform in the beginning. In the recommended design, it has been designed in two parts which make assembly easier. Therefore, thanks to the push-in pull-out characteristic the assembly of the replacement part will be done easily.

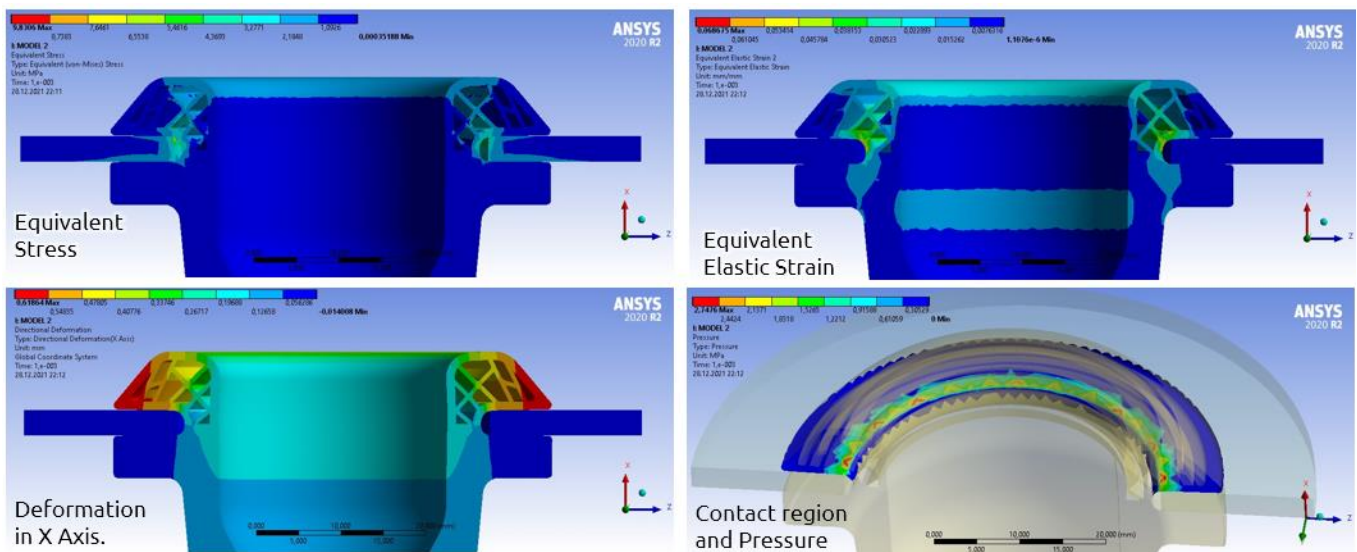


Fig. 18. Results of the stress-strain analysis using FEM for the replacement part schematically shown in Fig. 9

Based on the results of FEM, a design offering the best compliance with the characteristics of the original part has been selected. In further steps, the replacement part was printed and successfully tested. Fig. 19 shows selected replacement parts view after printing.

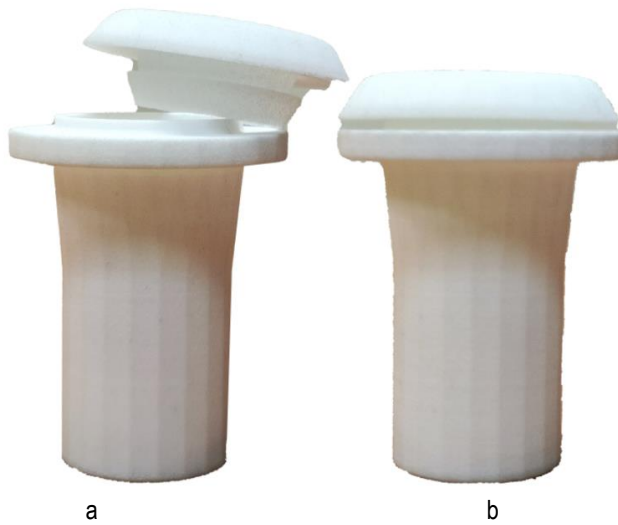


Fig. 19. Printed view of FEM based designed part; a) before assembly, b) after assembly

5. CONCLUSIONS

The results presented in the paper demonstrate an efficient approach to the fabrication of parts using efficient materials substituting the ones used in manufacturing of the originals. The approach adopted here can be summarized with the following points.

- The textile machine part that was strategically important was designed by following the RE application procedure, and has been manufactured by AM successfully.
- In the current case, the key characteristic is the asymmetric push-in pull-out characteristic of the part. By using this characteristic, the replacement part has been designed accordingly and hence, the assembly of the part became more easier.
- Selection of replacement material suitable for 3D printing of the part is accomplished and further exploring mechanical properties of the elements printed into fully dense and porous structures were made. Thus, adding geometrical features i.e. lattice structure in some regions, provided less stiffness on the part.
- Tensile and compression tests of TPU material have been conducted to characterize the mechanical properties and the obtained results have been adopted in FEA software and validated.
- The designed replacement part was subjected to FEA in order to analyse the stresses that will be encountered after the assembly. Thus, in accordance with the FEA performance, the stresses developed were observed and concluded there will be no failure after the assembly.
- The printing time is 2 h and the printing cost is c.a.15 USD.
- Finally, the replacement part has been fabricated by an SLS 3D printer and tested. It has been validated as it works properly onsite.

REFERENCES

1. The 3R Initiative, <https://www.env.go.jp/recycle/3r/en/outline.html> (accessed March 11, 2022).
2. Peng S, Ping J, Li T, et al. Environmental benefits of remanufacturing mechanical products: a harmonized meta-analysis of comparative life cycle assessment studies. *Journal of Environmental Management*; 306. 2022. DOI: 10.1016/J.JENVMAN.2022.114479.
3. Geng Z, Sabbaghi A, Bidanda B. Reconstructing Original Design: Process Planning for Reverse Engineering. DOI: 10.1080/24725854.2022.2040761.
4. Shahrubudin N, Lee TC, Ramlan R. An Overview on 3D Printing Technology: Technological, Materials, and Applications. *Procedia Manufacturing* 2019;35:1286–1296.
5. Harris CG, Jursik NJS, Rochefort WE, et al. Additive Manufacturing With Soft TPU – Adhesion Strength in Multimaterial Flexible Joints. *Front Mech Eng* 2019;5:37.
6. Xiao J, Gao Y. The manufacture of 3D printing of medical grade TPU. *Progress in Additive Manufacturing* 2017;3:117–123.
7. Haryńska A, Gubanska I, Kucinska-Lipka J, et al. Fabrication and Characterization of Flexible Medical-Grade TPU Filament for Fused Deposition Modeling 3DP Technology. *Polymers (Basel)*; 10. Epub ahead of print November 25, 2018. DOI: 10.3390/POLYM10121304.
8. Herzberger J, Sirrine JM, Williams CB, et al. Polymer Design for 3D Printing Elastomers: Recent Advances in Structure, Properties, and Printing. *Progress in Polymer Science* 2019;97:101144.
9. Rodríguez-Parada L, de la Rosa S, Mayuet PF. Influence of 3D-Printed TPU Properties for the Design of Elastic Products. *Polymers (Basel)* 2021;13:2519.
10. American Chemistry Council. Thermoplastic Polyurethanes Bridge the Gap between Rubber and Plastics, <https://www.americanchemistry.com/industry-groups/center-for-the-polyurethanes-industry-cpi/resources/library/thermoplastic-polyurethanes-bridge-the-gap-between-rubber-and-plastics> (2002, accessed January 17, 2022).
11. Xu T, Shen W, Lin X, et al. Mechanical properties of additively manufactured thermoplastic polyurethane (TPU) material affected by various processing parameters. *Polymers (Basel)* 2020;12:1–16.
12. Lee H, Eom RI, Lee Y. Evaluation of the mechanical properties of porous thermoplastic polyurethane obtained by 3D printing for protective gear. *Advances in Materials Science and Engineering*; 2019. Epub ahead of print 2019. DOI: 10.1155/2019/5838361.
13. Lu QW, Macosko CW, Horion J. Compatibilized blends of thermoplastic polyurethane (TPU) and polypropylene. *Macromolecular Symposia* 2003;198:221–232.
14. Mi HY, Salick MR, Jing X, et al. Characterization of thermoplastic polyurethane/polylactic acid (TPU/PLA) tissue engineering scaffolds fabricated by microcellular injection molding. *Materials Science and Engineering: C* 2013;33:4767–4776.
15. Li W, Liu J, Hao C, et al. Interaction of thermoplastic polyurethane with polyamide 1212 and its influence on the thermal and mechanical properties of TPU/PA1212 blends. *Polymer Engineering & Science* 2008;48:249–256.
16. Feng F, Ye L. Morphologies and mechanical properties of polylactide/thermoplastic polyurethane elastomer blends. *Journal of Applied Polymer Science* 2011;119:2778–2783.
17. Rodríguez L, Naya G, Bienvenido R. Study for the selection of 3D printing parameters for the design of TPU products. *IOP Conference Series: Materials Science and Engineering* 2021;1193:012035.
18. Schmid M, Amado A, Wegener K. Polymer powders for selective laser sintering (SLS). *AIP Conference Proceedings*; 1664. Epub ahead of print May 22, 2015. DOI: 10.1063/1.4918516.
19. Lupone F, Padovano E, Casamento F, et al. Process Phenomena and Material Properties in Selective Laser Sintering of Polymers: A Review. *Materials* 2022, 2021;15:183.
20. Shen F, Yuan S, Guo Y, et al. Energy Absorption of Thermoplastic Polyurethane Lattice Structures via 3D Printing: Modeling and Prediction. *International Journal of Applied Mechanics*; 8. Epub ahead of print 2016. DOI: 10.1142/S1758825116400068.

21. Kanbur Y, Tayfun U. Development of multifunctional polyurethane elastomer composites containing fullerene: Mechanical, damping, thermal, and flammability behaviors. *Journal of Elastomers and Plastics* 2019;51:262–279.
22. Beloshenko V, Beygelzimer Y, Chishko V, et al. Mechanical properties of flexible tpu-based 3d printed lattice structures: Role of lattice cut direction and architecture. *Polymers (Basel)* 2021;13:1–11.
23. Ursini C, Collini L. Fdm layering deposition effects on mechanical response of tpu lattice structures. *Materials*; 14. Epub ahead of print 2021. DOI: 10.3390/ma14195645.
24. Beloshenko V, Beygelzimer Y, Chishko V, et al. Mechanical Properties of Thermoplastic Polyurethane-Based Three-Dimensional-Printed Lattice Structures: Role of Build Orientation, Loading Direction, and Filler. *3D Printing and Additive Manufacturing* 2021; 3dp.2021.0031.
25. Ponticelli GS, Tagliaferri F, Venettacci S, et al. Re-Engineering of an Impeller for Submersible Electric Pump to Be Produced by Selective Laser Melting. *Applied Sciences* 2021, Vol 11, Page 7375 2021;11: 7375.
26. Hernández F, Fragoso A. Fabrication of a Stainless-Steel Pump Impeller by Integrated 3D Sand Printing and Casting: Mechanical Characterization and Performance Study in a Chemical Plant. *Applied Sciences* 2022;12:3539.
27. Zglobicka I, Chmielewska A, Topal E, et al. 3D Diatom–Designed and Selective Laser Melting (SLM) Manufactured Metallic Structures. *Scientific Reports*. 2019;9:1–9.
28. Zaoui M, Mohamad BA, Amroune S, et al. Manufacturing of rapid prototypes of mechanical parts using reverse engineering and 3D Printing. *J Serbian Soc Comput Mech* 2021;15:1–10.
29. Subeshan B, Abdulaziz A, Khan Z, et al. Reverse Engineering of Aerospace Components Utilizing Additive Manufacturing Technology. 2022;238–246.
30. Goodridge RD, Tuck CJ, Hague RJM. Laser sintering of polyamides and other polymers. *Progress in Materials Science* 2012;57:229–267.
31. Gueche YA, Sanchez-Ballester NM, Cailleaux S, et al. Selective Laser Sintering (SLS), a New Chapter in the Production of Solid Oral Forms (SOFs) by 3D Printing. *Pharmaceutics*. 2021; 13: 1212.
32. Tagliaferri V, Trovalusci F, Guarino S, et al. Environmental and Economic Analysis of FDM, SLS and MJF Additive Manufacturing Technologies. *Materials*. 2019;12:4161.
33. Kellens K, Renaldi R, Dewulf W, et al. Environmental impact modeling of selective laser sintering processes. *Rapid Prototyping Journal* 2014;20:459–470.
34. ISO527-2: Plastics — Determination of tensile properties — Part 2: Test conditions for moulding and extrusion plastics. *International Standard*.
35. ISO 7743: Rubber, vulcanized or thermoplastic — Determination of compression stress-strain properties. *International Standard*; 2017.
36. Bates SRG, Farrow IR, Trask RS. Compressive behaviour of 3D printed thermoplastic polyurethane honeycombs with graded densities. *Materials and Design* 2019;162:130–142.
37. Additive Manufacturing solutions & industrial 3D printer by EOS, <https://www.eos.info/en> (accessed January 18, 2022).
38. [Technology Applied - Zaufany dostawca części dla przemysłu, <https://ta.parts/> (accessed January 18, 2022).
39. EOS. Thermoplastisches Polyurethan EOS TPU 1301, https://webcache.googleusercontent.com/search?q=cache:90GEoHlUXOwJ:https://www.eos.info/03_system-related-assets/material-related-contents/polymer-materials-and-examples/tpu-1301/material_datasheet_eos_tpu_1301_core_de_web.pdf+&cd=3&hl=tr&ct=clnk&gl=pl&cl (accessed January 11, 2022).

Mehmet Aladag:  <https://orcid.org/0000-0002-2484-7519>

Monika Bernacka:  <https://orcid.org/0000-0003-3481-0768>

Magdalena Joka-Yildiz:  <https://orcid.org/0000-0002-4745-5972>

Wojciech Grodzki:  <https://orcid.org/0000-0002-0068-9683>

Przemysław Zamojski:  <https://orcid.org/0000-0002-3736-8840>

Izabela Zglobicka:  <https://orcid.org/0000-0002-4432-9196>